Research Square

Preprints are preliminary reports that have not undergone peer review.
They should not be considered conclusive, used to inform clinical practice,
or referenced by the media as validated information.

Distinct Predictive and Recovery EEG Biomarkers of Motor Function after Noninvasive Brain Stimulation in Subacute Stroke Patients

Hyejeong Han
The Catholic University of Korea
Yerim Huh
The Catholic University of Korea
Sang Wook Lee
The Catholic University of America
Yun-Hee Kim
Myongji Choonhey Rehabilitation Hospital
Minji Lee
minjilee@catholic.ac.kr

The Catholic University of Korea

Research Article

Keywords: Stroke, Noninvasive brain stimulation, Electroencephalography, Motor recovery, EEG biomarkers, Neuroplasticity, Longitudinal analysis

Posted Date: May 15th, 2026

DOI: https://doi.org/10.21203/rs.3.rs-9648366/v1

License: This work is licensed under a Creative Commons Attribution 4.0 International License.
Read Full License

Additional Declarations: No competing interests reported.

Distinct Predictive and Recovery EEG Biomarkers of Motor Function after Noninvasive Brain Stimulation in Subacute Stroke Patients

Hyejeong Han[1], Yerim Huh[2], Sang Wook Lee[3], Yun-Hee Kim[4,5], Minji Lee[2,6*]

[1]School of Information, Communications and Electronics Engineering, The Catholic University of Korea, Bucheon, Gyeonggi 14662, South Korea.

[2]Department of Healthcare and Artificial Intelligence, The Catholic University of Korea, Bucheon, Gyeonggi 14662, South Korea.

[3]Department of Biomedical Engineering, The Catholic University of America, Washington, DC, 20064-0001, USA.

[4]Myongji Choonhey Rehabilitation Hospital, Seoul, 07378, South Korea.

[5]Department of Physical and Rehabilitation Medicine, Sungkyunkwan University School of Medicine, Seoul, 06351, South Korea.

[6]Department of Biomedical Software Engineering, The Catholic University of Korea, Bucheon, Gyeonggi 14662, South Korea.

*Corresponding author(s). E-mail(s): minjilee@catholic.ac.kr;

Abstract

Background: Electroencephalography (EEG) has emerged as a promising biomarker for predicting motor recovery in stroke patients undergoing non-invasive brain stimulation (NIBS), including repetitive transcranial magnetic stimulation and transcranial direct current stimulation. However, it remains unclear whether baseline EEG features that account for between-subject variability in treatment responsiveness also capture within-subject neural changes associated with motor recovery over time. This study investigated whether predictive EEG biomarkers and recovery-related EEG changes represent distinct neural mechanisms.

Methods: Twelve patients with subacute stroke received dual-mode NIBS and were classified as responders ($\boldsymbol{n = 7}$) or non-responders ($\boldsymbol{n = 5}$) based on changes in the Fugl–Meyer Assessment Upper Extremity (FMA-UE) score two

months after stimulation. Baseline EEG features, including power spectral density (PSD), phase-locking value (PLV), and coherence (COH), were used to train multiple machine learning models to predict treatment responsiveness. Model performance was evaluated using 10-fold cross-validation. Longitudinal statistical analyses were conducted to examine associations between EEG changes across visits and motor recovery.
Results: PSD-based models achieved the highest classification performance, with LightGBM yielding the best overall accuracy. Permutation importance analysis identified beta-band power at the ipsilesional T3 channel as the most influential baseline feature. In contrast, longitudinal analyses revealed a distinct pattern. Only changes in relative spectral power were significantly associated with motor recovery, with relative delta power changes at the ipsilesional O1 channel showing a significant correlation with improvements in FMA-UE scores ($\boldsymbol{p < 0.05}$). No significant associations were observed for absolute or log-transformed power measures.
Conclusions: Baseline treatment responsiveness and subsequent motor recovery were characterized by distinct neurophysiological signatures. Beta-band power at the ipsilesional T3 region may serve as a predictive biomarker of treatment response, whereas longitudinal changes in relative delta power at the ipsilesional O1 region were associated with recovery-related cortical reorganization. These findings support a framework that distinguishes predictive biomarkers from recovery-tracking biomarkers and may improve the interpretability of EEG-based prognostic models for stroke rehabilitation.
Trial registration: Not applicable.

Keywords: Stroke, Noninvasive brain stimulation, Electroencephalography, Motor recovery, EEG biomarkers, Neuroplasticity, Longitudinal analysis

1 Introduction

Stroke is one of the leading causes of long-term disability worldwide and frequently results in persistent motor impairment after the acute phase [1]. Predicting motor recovery remains a major challenge in neurorehabilitation, as clinical outcomes vary substantially among patients with similar initial impairments. Increasing attention has therefore been directed toward identifying neurophysiological markers that reflect central nervous system reorganization during recovery [2]. Non-invasive brain stimulation (NIBS), including repetitive transcranial magnetic stimulation (rTMS) and transcranial direct current stimulation (tDCS), has been widely investigated as a therapeutic approach to promote post-stroke motor recovery by modulating cortical excitability and facilitating neuroplasticity [3–6]. Recent studies suggest that the conventional motor hot-spot may not represent the optimal stimulation site, and that individualized electrode positioning based on current distribution may enhance stimulation efficacy [7]. At the same time, electroencephalography (EEG) has emerged as a practical and cost-effective tool for characterizing brain activity and identifying biomarkers associated with functional recovery in stroke rehabilitation [8, 9]. Machine learning–based EEG classification frameworks have also been explored in stroke rehabilitation, and

previous studies have demonstrated the feasibility of cross-subject analysis despite substantial inter-subject variability [10].

Previous studies have shown that various EEG-derived features, particularly spectral power in specific frequency bands, are associated with motor impairment and functional recovery after stroke [11]. Power spectral density (PSD) has been linked to long-term motor recovery in patients with subacute stroke and has emerged as a potential prognostic biomarker. Machine learning approaches have increasingly been applied to EEG data for predicting treatment responsiveness and clinical outcomes. EEG features, including spectral power and functional connectivity measures, have shown promising classification performance across stroke rehabilitation studies [12]. Connectivity metrics such as phase locking value (PLV) and coherence (COH) have also been widely used to characterize functional interactions between brain regions in EEG-based analyses. Despite these advances, the clinical interpretability of EEG-based predictive models remains limited. Many studies have focused primarily on predictive accuracy, whereas the neurophysiological significance of the features driving model performance remains unclear. Consequently, it remains unclear whether baseline EEG features that account for between-subject variability in treatment responsiveness also capture within-subject neural changes associated with motor recovery over time.

Most existing studies have focused either on predicting clinical outcomes at baseline or on longitudinal monitoring of recovery using EEG indicators [13]. EEG-based biomarkers also vary considerably across studies and lack standardized metrics, making it difficult to interpret and compare findings across different experimental settings [14]. Consequently, studies that directly compare predictive analysis and longitudinal monitoring using the same EEG features remain limited. These two analytical approaches address fundamentally different clinical questions. Predictive analysis aims to identify patients who are likely to achieve favorable clinical outcomes, whereas longitudinal analysis seeks to characterize neurophysiological changes associated with functional recovery over time. Whether a single EEG biomarker can support both prediction and recovery monitoring, or whether distinct biomarkers are required for each purpose, remains unclear.

Most EEG studies in stroke rehabilitation have primarily relied on absolute power measurements. Although absolute power reflects overall signal amplitude, it is highly sensitive to inter-individual variability and global scaling effects, making comparisons across patients more challenging [15]. As stroke rehabilitation increasingly emphasizes individualized recovery trajectories, EEG metrics that are robust to inter-subject variability are needed. Relative spectral power and its longitudinal changes may provide a more informative representation of cortical reorganization because they capture the redistribution of spectral energy across frequency bands rather than absolute signal magnitude. However, the relative clinical relevance of absolute, log-transformed, and relative power measures for characterizing motor recovery remains insufficiently understood. In addition, conventional power-based spectral measures may be influenced by aperiodic background activity, which may further complicate the interpretation of longitudinal EEG changes [16].

In this study, we investigated whether baseline EEG features that predict treatment responsiveness also capture longitudinal neural changes associated with motor

recovery following NIBS in patients with subacute stroke. Machine learning–based classification using baseline EEG features was combined with longitudinal statistical analysis of EEG spectral changes across multiple visits. In particular, absolute, log-transformed, and relative power spectral density measures were systematically compared to determine which spectral representation is most strongly associated with motor recovery. We hypothesized that predictive biomarkers and recovery-related EEG changes would exhibit distinct neurophysiological signatures. Distinguishing baseline predictive markers from longitudinal recovery-tracking biomarkers may provide new insight into the neural mechanisms underlying post-stroke motor recovery.

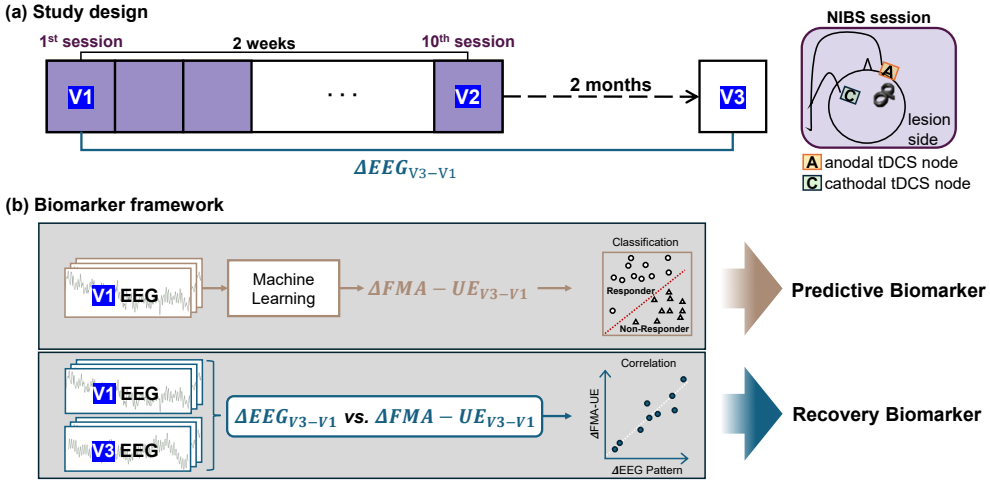


Fig. 1 Overview of the study design and analysis framework. (a) Study design. Participants underwent non-invasive brain stimulation (NIBS) once daily on weekdays for two consecutive weeks (10 sessions). EEG and motor function (FMA−UE) were assessed at three time points: before the first NIBS session (Visit 1, V1), after the final NIBS session (Visit 2, V2), and at a 2-month follow-up (Visit 3, V3). (b) Biomarker framework. Baseline EEG recorded at V1 was used for machine learning–based classification to predict treatment responsiveness, defined by changes in FMA−UE between V3 and V1. The classification plot illustrates the decision boundary separating responders and non-responders. In parallel, longitudinal changes in EEG (ΔEEG, V3−V1) were correlated with changes in motor function (ΔFMA-UE, V3−V1). The regression plot represents the continuous association between EEG changes and motor recovery. This framework distinguishes predictive biomarkers derived from baseline EEG from recovery biomarkers reflecting longitudinal neural changes.

2 Methods

The overall analysis framework is illustrated in Fig. 1. Baseline EEG features acquired at Visit 1 were used to train machine learning models to predict treatment responsiveness. In parallel, longitudinal EEG data from Visit 1 to Visit 3 were analyzed to examine neurophysiological changes associated with motor recovery.

Table 1 Clinical characteristics of the 12 subacute stroke patients.

No	Sex	Age	Lesion	Baseline FMA-UE	ΔFMA-UE	Group
P-001	M	56	Lt. paramedian pons infarction	41	21	R
P-002	F	72	Rt. CR infarction	35	21	R
P-003	M	59	Lt. pons infarction	29	14	R
P-004	M	71	Rt. paramedian pons infarction	34	24	R
P-005	F	64	Rt. pons infarction	50	13	R
P-006	M	47	Lt. MCA infarction	17	26	R
P-007	F	53	Rt. thalamus infarction (PCA)	58	2	NR
P-008	M	75	Rt. SC infarction	60	-2	NR
P-009	M	66	Rt. MCA infarction	44	11	NR
P-010	M	54	Rt. borderzone infarction	16	14	R
P-011	M	63	Lt. CR infarction	24	-3	NR
P-012	M	46	Lt. BG ICH	5	-1	NR
Mean ± SD		60.5 ± 9.4		34.4 ± 17.0	11.7 ± 10.4	

Note: ΔFMA-UE = V3 − V1. R, responder; NR, non-responder. Lesion abbreviations: Lt., left; Rt., right; CR, corona radiata; MCA, middle cerebral artery; PCA, posterior cerebral artery; SC, subcortical; BG, basal ganglia; ICH, intracerebral hemorrhage.

2.1 Participants

This study included 12 patients with subacute stroke who underwent EEG recordings and NIBS as part of a rehabilitation protocol. The study was approved by the Institutional Review Board of Samsung Medical Center (approval no. SMC 2013-06-002). All experimental procedures were conducted in accordance with the relevant guidelines and regulations, and written informed consent was obtained from all participants or their legal guardians. Clinical characteristics of the study participants are summarized in Table 1.

Following brain injury, behavior is often altered, reflecting substantial changes in experiential and adaptive processes [17]. Accordingly, patients were classified as responders or non-responders based on changes in the Fugl–Meyer Assessment Upper Extremity (FMA-UE) score. Treatment response was defined as an improvement of 13 points or more between baseline and the two-month follow-up. As the minimal clinically important difference for the FMA-UE varies across studies depending on patient characteristics, baseline impairment severity, and the anchor used, previously reported thresholds range from approximately 9 to 13 points [18]. In the present study, we adopted a 13-point threshold as a conservative criterion to identify clinically meaningful improvement, thereby reducing the likelihood of classifying marginal changes as treatment response in this small cohort. According to this definition, the responder group consisted of seven patients (mean age 60.43 ± 9.14 years; two females), and the non-responder group consisted of five patients (mean age 60.6 ± 11.33 years; one female). The mean ΔFMA-UE was higher in responders (19.0 ± 5.29) than in non-responders (1.4 ± 5.68).

2.2 Experimental Protocol

EEG recordings and clinical assessments were performed at three time points (Visit 1–Visit 3). Visit 1 was conducted approximately two weeks after stroke onset, prior to the initiation of NIBS. Following baseline assessment, all patients underwent a dual-mode brain stimulation protocol combining rTMS and tDCS. Stimulation sessions were administered on weekdays for two consecutive weeks, resulting in a total of 10 sessions. Visit 2 was performed immediately after completion of the stimulation sessions, and Visit 3 was conducted two months after the end of stimulation without additional intervention. Clinical outcomes at Visit 3 were used to evaluate long-term treatment effects.

Dual-mode stimulation was delivered using a simultaneous protocol targeting the primary motor cortex (M1). The stimulation target corresponded to the M1 region associated with the affected upper limb. Excitatory rTMS was applied to the ipsilesional M1 at 10 Hz with an intensity of 90% of the resting motor threshold. Stimulation was delivered in 5-second trains separated by 55-second inter-train intervals, resulting in 1,000 pulses per session. Concurrently, cathodal tDCS was applied to the contralesional M1 for 20 minutes to suppress interhemispheric inhibition.

For machine learning–based prediction, only baseline EEG data obtained at Visit 1 were used to train models for predicting treatment responsiveness. In contrast, EEG data collected from Visit 1 to Visit 3 were used for longitudinal statistical analyses to examine neurophysiological changes associated with motor recovery.

2.3 EEG Acquisition

Detailed clinical characteristics of the participants are provided in Supplementary Table 1. EEG recordings were obtained at three predefined time points: before the first stimulation session (Visit 1, V1), after completion of the stimulation protocol (Visit 2, V2), and at a 2-month follow-up (Visit 3, V3). EEG data were recorded during resting-state with eyes closed for 5 minutes at each visit. Participants were instructed to remain relaxed and minimize movement during recording. Recordings were acquired using either a 27-channel system with a sampling rate of 500 Hz or 11- and 12-channel systems with a sampling rate of 128 Hz, depending on the visit and patient. To ensure consistency across recordings, analyses were restricted to a common subset of EEG channels available across configurations. Signals were resampled and standardized for consistent feature extraction. Continuous EEG signals were segmented into non-overlapping 5-second epochs, resulting in approximately 60 trials per recording session. Epochs containing excessive artifacts ($\pm 100\ \mu$V) were excluded from further analysis. Detailed information on the EEG acquisition protocol and stimulation procedures has been described previously [19, 20].

2.4 EEG Preprocessing

All EEG recordings were preprocessed to ensure consistency across subjects and recording configurations. To account for lesion-side differences, EEG channels were spatially aligned such that the lesioned hemisphere was consistently mapped to the

left hemisphere for all subjects. The EEG signals were band-pass filtered between 1 and 30 Hz to remove slow drifts and high-frequency noise.

Independent component analysis (ICA) was applied to remove ocular and muscle artifacts. The cleaned EEG signals were then segmented into 5-s epochs for subsequent analysis [21]. For spectral analysis, the signals were analyzed within four conventional frequency bands [22]: delta (δ, 1–4 Hz), theta (θ, 4–8 Hz), alpha (α, 8–13 Hz), and beta (β, 13–30 Hz). Gamma-band activity was not analyzed because high-frequency scalp EEG signals are highly susceptible to contamination from muscle artifacts [23]. In stroke-related motor recovery studies, oscillatory activity in lower frequency bands (delta to beta) has been more consistently associated with sensorimotor processing and clinical outcomes [24, 25]. Accordingly, the analysis was restricted to delta-to-beta frequency bands, which are widely used and well validated in clinical resting-state EEG studies of motor function and neurorehabilitation.

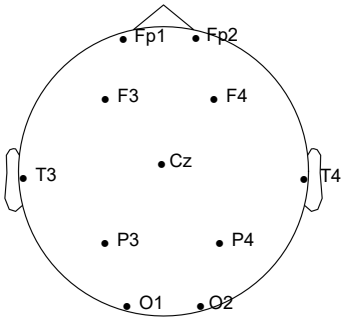


Fig. 2 Electrode layout of the 11 EEG channels used for analysis. Analyses were restricted to a common subset of channels available across different EEG acquisition configurations.

As summarized in Supplementary Table 1, EEG recordings were acquired using two configurations with either 27 channels or 11 channels. To ensure inter-subject consistency, analyses were restricted to a common subset of 11 channels (Fp1, Fp2, F3, F4, T3, Cz, T4, P3, P4, O1, and O2) available in all recordings (Fig. 2; Supplementary Table S1). Finally, all EEG data were downsampled to 128 Hz to standardize the sampling frequency across the dataset.

2.5 Feature Extraction

Three types of EEG features were extracted to characterize neural activity and functional connectivity: PSD, PLV, and COH. These features capture complementary aspects of brain dynamics, including local spectral activity and inter-regional synchronization.

2.5.1 Power Spectral Density

PSD was estimated for each epoch and channel using Welch's method. Within each epoch, the EEG signal was segmented into overlapping windows of 0.5 s with

50% overlap, and the resulting spectral estimates were averaged to obtain a stable representation of the frequency content.

Band-specific spectral power was calculated by integrating the PSD within four conventional frequency bands: delta (δ, 1–4 Hz), theta (θ, 4–8 Hz), alpha (α, 8–13 Hz), and beta (β, 13–30 Hz). The absolute band power for band b was defined as

$$P_b = \int_{f \in b} \mathrm{PSD}(f)\, df \tag{1}$$

where $\mathrm{PSD}(f)$ denotes the estimated power spectral density at frequency f. These absolute band powers were used to characterize local spectral activity.

In addition to absolute PSD, two normalized spectral representations were derived: log-transformed PSD and relative PSD. The log-transformed band power was computed as

$$P_b^{\log} = \log(P_b) \tag{2}$$

Relative PSD was obtained by normalizing each band power by the total power across all considered frequency bands:

$$P_b^{\mathrm{rel}} = \frac{P_b}{\sum_{k \in \{\delta,\theta,\alpha,\beta\}} P_k} \tag{3}$$

This representation emphasizes the relative spectral composition of the signal and reduces sensitivity to global amplitude scaling, enabling more robust comparisons across subjects and across longitudinal recordings.

2.5.2 Phase-Locking Value

Phase synchronization between EEG channels was quantified using the PLV. For each 5-s epoch, band-limited EEG signals were obtained for the four frequency bands described above. The instantaneous phase of each signal was estimated using the analytic signal derived from the Hilbert transform. The PLV between channels i and j was computed as

$$\mathrm{PLV}_{ij} = \left| \frac{1}{N} \sum_{n=1}^{N} \exp\big(j\big(\phi_i(n) - \phi_j(n)\big)\big) \right| \tag{4}$$

where $\phi_i(n)$ and $\phi_j(n)$ denote the instantaneous phases of channels i and j at sample n, and N is the number of samples within the epoch. PLV ranges from 0 to 1, where larger values indicate stronger phase synchronization between signals.

To obtain node-wise connectivity features, a degree-like measure was computed by averaging the pairwise PLV values between channel i and all other channels:

$$\deg_i = \frac{1}{C-1} \sum_{\substack{j=1 \\ j \neq i}}^{C} \mathrm{PLV}_{ij} \tag{5}$$

where C is the number of channels. This degree feature summarizes the overall phase synchronization strength of each channel with respect to the rest of the network.

Degree values were calculated for each frequency band and concatenated to form the final PLV-based feature vector.

2.5.3 Coherence

Frequency-domain functional connectivity was evaluated using magnitude-squared COH. For each 5-s epoch, coherence between EEG channels i and j was computed as

$$\mathrm{COH}_{ij}(f) = \frac{|S_{ij}(f)|^2}{S_{ii}(f)\, S_{jj}(f)} \tag{6}$$

where $S_{ii}(f)$ and $S_{jj}(f)$ denote the auto-spectral densities of the signals and $S_{ij}(f)$ denotes their cross-spectral density at frequency f. COH ranges from 0 to 1, where higher values indicate stronger linear coupling between signals at a given frequency.

Band-specific coherence was obtained by averaging $\mathrm{COH}_{ij}(f)$ across the frequency bins belonging to each band. To obtain node-wise connectivity features, a degree-like measure was computed by averaging the band-specific coherence between channel i and all other channels:

$$\deg_i^{(b)} = \frac{1}{C-1} \sum_{\substack{j=1 \\ j \neq i}}^{C} \overline{\mathrm{COH}}_{ij}^{(b)} \tag{7}$$

where C is the number of channels. This feature summarizes the overall coherence-based connectivity strength of each channel within frequency band b. Degree features were calculated for each band and concatenated to form the final COH-based feature vector.

2.6 Between-Subject Classification Analysis

Machine learning models were trained to classify treatment responsiveness using baseline EEG features obtained at Visit 1 (pre-NIBS). The input features consisted of spectral power, phase synchronization, and coherence measures (PSD, PLV, and COH). Models were trained using individual feature sets as well as combined feature representations. Target labels were defined based on longitudinal changes in motor function, quantified as the difference in FMA-UE scores between Visit 3 and Visit 1 (ΔFMA-UE).

Five classifiers were evaluated: support vector machine (SVM), L1-regularized logistic regression (L1-LogReg), linear discriminant analysis (LDA), extreme gradient boosting (XGBoost), and light gradient boosting machine (LightGBM). Linear models were included as baseline classifiers, whereas gradient boosting models were evaluated to capture potentially nonlinear relationships within EEG features.

Model performance was evaluated using stratified 10-fold cross-validation to obtain a robust estimate of generalization performance and to reduce the risk of overfitting. The dataset was partitioned into ten folds while preserving the class distribution. In each iteration, nine folds were used for training and one fold was used for testing, ensuring that samples in the test fold were not used during model training. All pre-processing steps, including feature standardization, were performed exclusively on the

training data within each fold and then applied to the corresponding test fold to prevent data leakage. This procedure was repeated until each fold served as the test set once.

Classification performance was assessed using accuracy, F1-score, and the area under the receiver operating characteristic curve (ROC-AUC). To improve the interpretability of the trained models, permutation-based feature importance analysis was performed to identify the EEG channels and frequency bands that contributed most strongly to prediction performance.

2.7 Within-Subject Longitudinal Correlation Analysis

Associations between EEG-derived features and changes in motor function were evaluated using Spearman's rank correlation coefficient. This non-parametric approach was chosen because of the small sample size and the potential non-normal distribution of the variables. Spearman correlation was used because it is robust to outliers and does not assume linear relationships. Correlation analyses were performed to assess the relationship between EEG measures and clinical outcomes, quantified as changes in the FMA-UE score.

To investigate longitudinal neurophysiological changes during rehabilitation, EEG features obtained across visits (Visit 1, Visit 2, and Visit 3) were examined and compared with corresponding changes in motor function. Additional analyses focused on PSD-based measures to evaluate spectral dynamics over time. Specifically, three spectral representations were considered: absolute PSD, log-transformed PSD changes (Δlog PSD), and relative PSD changes (Δrelative PSD). These measures were used to examine how spectral power redistribution across frequency bands was associated with motor recovery. Statistical significance was assessed using a threshold of $p < 0.05$.

3 Results

3.1 Baseline EEG predictors of treatment response

Table 2 summarizes the classification performance of five classifiers using baseline EEG feature types (PSD, Δlog PSD, Δrelative PSD, PLV, and COH), evaluated with stratified 10-fold cross-validation. Across classifiers, PSD-based features consistently outperformed connectivity-based features (PLV and COH) in terms of accuracy, F1-score, and ROC-AUC. Among the tested models, LightGBM with PSD features achieved the best overall performance, with an accuracy of 0.986 ± 0.015 and an F1-score of 0.987 ± 0.013. XGBoost with PSD features achieved the highest ROC-AUC (0.998 ± 0.002), which was comparable to that of LightGBM (0.998 ± 0.004). These results indicate similarly strong discriminative performance between the two gradient boosting models.

Log-transformed PSD features showed performance comparable to that of absolute PSD features across most models. This pattern was particularly evident in tree-based classifiers, including XGBoost and LightGBM. In contrast, models trained with PLV and COH features consistently showed lower performance across all evaluation metrics.

These findings suggest that baseline spectral power features provide more discriminative information for predicting treatment responsiveness than connectivity-based features in this dataset. Based on the overall performance and stability across metrics, LightGBM with PSD features was selected as the final model for subsequent analyses.

Table 2 Baseline classification performance across EEG feature types.

Model	Feature	Accuracy	F1-score	ROC-AUC
SVM	PSD	0.881 ± 0.033	0.886 ± 0.031	0.956 ± 0.026
	log PSD	0.929 ± 0.030	0.935 ± 0.027	0.983 ± 0.015
	relative PSD	0.887 ± 0.030	0.896 ± 0.030	0.946 ± 0.022
	PLV	0.830 ± 0.039	0.837 ± 0.040	0.904 ± 0.017
	COH	0.796 ± 0.029	0.807 ± 0.029	0.892 ± 0.029
L1-LogReg	PSD	0.884 ± 0.035	0.888 ± 0.035	0.961 ± 0.023
	log PSD	0.933 ± 0.028	0.938 ± 0.026	0.983 ± 0.013
	relative PSD	0.882 ± 0.034	0.893 ± 0.031	0.948 ± 0.021
	PLV	0.830 ± 0.032	0.841 ± 0.029	0.912 ± 0.017
	COH	0.798 ± 0.037	0.809 ± 0.036	0.897 ± 0.025
LDA	PSD	0.862 ± 0.040	0.863 ± 0.044	0.956 ± 0.031
	log PSD	0.938 ± 0.030	0.943 ± 0.028	0.984 ± 0.012
	relative PSD	0.878 ± 0.025	0.893 ± 0.021	0.943 ± 0.021
	PLV	0.834 ± 0.036	0.842 ± 0.037	0.910 ± 0.019
	COH	0.825 ± 0.041	0.838 ± 0.037	0.897 ± 0.025
XGBoost	PSD	0.977 ± 0.015	0.979 ± 0.013	$\mathbf{0.998 \pm 0.002}$
	log PSD	0.977 ± 0.015	0.979 ± 0.013	$\mathbf{0.998 \pm 0.002}$
	relative PSD	0.963 ± 0.024	0.966 ± 0.022	0.994 ± 0.005
	PLV	0.871 ± 0.038	0.885 ± 0.034	0.954 ± 0.019
	COH	0.851 ± 0.036	0.866 ± 0.031	0.928 ± 0.021
LightGBM	PSD	$\mathbf{0.986 \pm 0.015}$	$\mathbf{0.987 \pm 0.013}$	0.998 ± 0.004
	log PSD	$\mathbf{0.986 \pm 0.015}$	$\mathbf{0.987 \pm 0.013}$	0.998 ± 0.004
	relative PSD	0.964 ± 0.022	0.967 ± 0.020	0.996 ± 0.004
	PLV	0.884 ± 0.028	0.897 ± 0.023	0.951 ± 0.021
	COH	0.856 ± 0.037	0.871 ± 0.032	0.935 ± 0.023

Note: Values are presented as mean ± standard deviation. Bold values indicate the highest performance for each metric (Accuracy, F1-score, ROC-AUC) across all models and feature types.

Permutation-based feature importance was assessed for the LightGBM model to identify the most influential baseline PSD features. The spatial distribution of feature importance across frequency bands (delta, theta, alpha, and beta) is shown in Fig. 3. Importance values were predominantly localized in temporal regions, with the strongest contribution observed in the beta band over the left temporal area. Consistent with these spatial patterns, the highest-ranked feature was T3 in the beta band (0.067 ± 0.078), followed by Fp2 in the beta band (0.032 ± 0.051) and O1 in the alpha band (0.020 ± 0.021). The ranking of top features is summarized in Table 3. Additional high-ranking features included O1-beta, Fp2-alpha, and T4-beta. Among the top-ranked features, beta-band power appeared most frequently, with selected alpha-band features also contributing to model performance. Band-wise aggregation showed that beta-band features contributed most strongly to model performance.

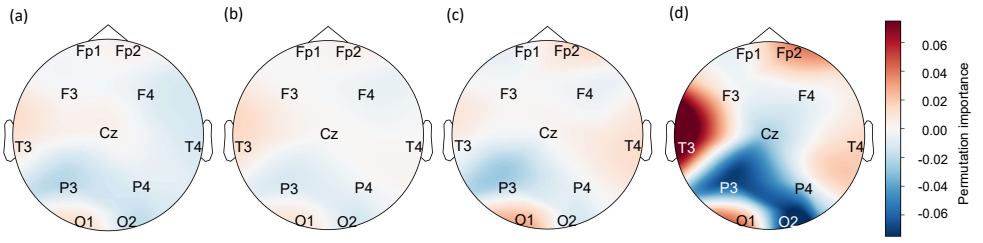


Fig. 3 Topographic distributions of permutation importance for baseline PSD features across frequency bands. (a) delta, (b) theta, (c) alpha, and (d) beta. Warmer colors indicate greater importance.

Delta-band features showed a moderate contribution, whereas the other frequency bands showed comparatively smaller effects. Channel-wise aggregation identified T3 as the most influential channel, with additional contributions from O1 and Fp2. This spatial pattern was consistent with the feature-level importance analysis.

Table 3 Top baseline PSD features ranked by permutation importance.

Feature (channel-band)	Importance (mean ± SD)
T3-beta	0.067 ± 0.078
Fp2-beta	0.032 ± 0.051
O1-alpha	0.020 ± 0.021
O1-beta	0.018 ± 0.164
Fp2-alpha	0.011 ± 0.009
T4-beta	0.011 ± 0.027
T3-theta	0.010 ± 0.012
T4-alpha	0.010 ± 0.028
O1-delta	0.007 ± 0.010
T3-delta	0.006 ± 0.008

Note: Values indicate permutation importance computed as the mean decrease in performance after feature permutation, averaged across epoch-stratified cross-validation folds.

3.2 Longitudinal EEG correlates of motor recovery

Correlations between longitudinal EEG changes and motor recovery were evaluated using Spearman's rank correlation between changes in Fugl–Meyer Assessment–Upper Extremity scores (ΔFMA-UE) and EEG features. To account for inter-individual variability in EEG power, three PSD representations were analyzed: absolute PSD, Δlog-PSD, and Δrelative PSD. Longitudinal changes were computed relative to Visit 1 (baseline), and comparisons were performed for Visit 2 (2 weeks) and Visit 3 (10 weeks).

When all patients were included, no statistically significant correlations were observed for any PSD representation at either Visit 2 or Visit 3. When the analysis was

restricted to patients classified as responders, significant correlations emerged only for the Δrelative PSD representation. At Visit 2, relative delta power changes between Visit 2 and Visit 1 showed no statistically significant association with ΔFMA-UE. In contrast, at Visit 3, relative delta power changes between Visit 3 and Visit 1 exhibited a strong negative correlation with ΔFMA-UE at O1 (Spearman's $\rho = -0.946$, $p = 0.0013$) and O2 ($\rho = -0.800$, $p = 0.0307$). Among these, only O1 and O2 reached statistical significance at the 10-week follow-up, while other channels (P3, T3, and F3) showed weaker, non-significant trends. No statistically significant correlations were observed for absolute PSD or Δlog PSD at any visit (Table 4).

The spatial distribution of correlation coefficients revealed a posterior-dominant pattern, with the strongest association localized over the O1 channel (Fig. 4). At the individual-subject level, the scatter plot showed a clear negative association between changes in relative delta power at O1 and motor recovery. Larger reductions in relative delta power were associated with greater improvements in FMA-UE scores.

Table 4 Spearman correlation between changes in relative PSD (Δrelative PSD) and motor recovery (ΔFMA-UE) in the responders (R).

Feature (channel-band)	Spearman ρ	p-value
O1-delta	-0.946	0.0013
O2-delta	-0.800	0.0307
P3-delta	-0.709	0.0743
T3-delta	-0.618	0.1389

Note: Δrelative PSD and ΔFMA-UE indicate changes between baseline and Visit 3 (10 weeks). Channels are ordered by ascending p-value.

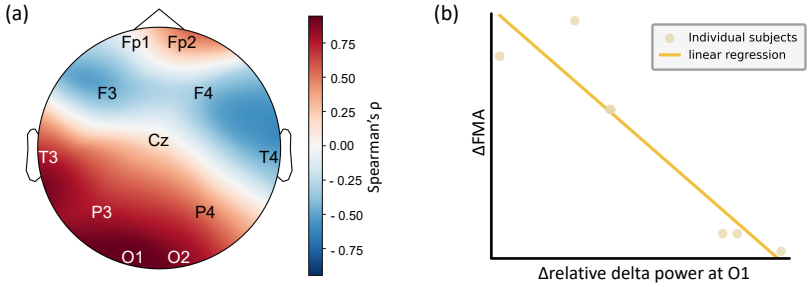


Fig. 4 Longitudinal EEG correlates of motor recovery based on changes in relative delta-band power. (a) Topographic distribution of Spearman correlation coefficients between changes in relative delta-band power (Visit 3 − Visit 1) and motor recovery (ΔFMA-UE) in the responders. Color intensity reflects the strength of the correlation, with more negative values indicating stronger associations. The strongest effect was observed over the O1 channel. (b) Scatter plot illustrating the relationship between changes in relative delta-band power at the O1 channel and ΔFMA-UE. The solid line represents the regression trend, indicating a significant negative association (Spearman's $\rho = -0.946$, $p = 0.0013$).

3.3 Distinct biomarkers for prediction and recovery

Baseline feature importance analysis showed that classification performance was primarily driven by beta-band activity in temporal and frontal regions. T3 and Fp2 were identified as the most influential baseline features. These features showed the highest contribution to distinguishing responders from non-responders. In contrast, the longitudinal analysis revealed a different pattern. Motor recovery was significantly associated only with changes in relative delta power. The strongest association was observed at O1, with a secondary effect at O2. No significant longitudinal associations were observed for beta-band features, including T3. These results indicate that the EEG features associated with baseline classification differed from those associated with longitudinal motor recovery.

4 Discussion

In this study, we investigated EEG-based biomarkers for predicting and interpreting motor recovery following NIBS in patients with subacute stroke by integrating machine learning with longitudinal statistical analysis. Baseline classification showed that spectral power features provided the most discriminative information for predicting treatment responsiveness. Across classifiers, spectral power features consistently outperformed connectivity-based measures such as PLV and coherence. This finding is consistent with previous studies reporting the prognostic utility of spectral power in stroke rehabilitation [11]. In contrast, connectivity-based measures showed lower classification performance in the present dataset. Previous studies have suggested that connectivity measures may be more susceptible to signal mixing and noise contamination, particularly in small clinical datasets [26, 27]. Feature importance analysis further identified beta-band activity in the temporal region, particularly at T3, as the most influential baseline feature. These findings support the use of PSD-derived features as a stable and interpretable representation for baseline prediction in stroke rehabilitation.

The machine learning analysis further highlighted the importance of beta-band activity in predicting treatment responsiveness in patients with subacute stroke. In the present study, beta-band activity at T3 was identified as the most influential feature in the baseline classification model. This finding is consistent with previous studies showing that beta oscillations are closely associated with motor function and sensorimotor integration [23]. Movement-related beta activity has also been associated with motor impairment and recovery after stroke, particularly in relation to Fugl–Meyer motor scores in subacute populations [28, 29]. Previous studies further demonstrated that neurophysiological measures of motor cortical function can predict rehabilitation outcomes [30]. Therefore, these findings suggest that beta-band activity in temporal–sensorimotor regions may serve as a clinically relevant biomarker for identifying patients who are more likely to benefit from NIBS.

In contrast to the baseline prediction results, the longitudinal analyses showed that recovery-related EEG changes were more strongly associated with relative spectral power than with absolute or log-transformed PSD measures. In the responder group, changes in relative delta power at O1 showed the strongest association with

improvements in FMA-UE scores. These findings indicate that longitudinal recovery is more closely reflected by dynamic spectral reorganization than by baseline power levels. Relative power metrics capture the redistribution of spectral energy across frequency bands and are less sensitive to inter-individual variability than absolute power measures [30]. This property makes relative PSD particularly suitable for tracking temporal changes in cortical activity. Relative power reflects frequency-specific shifts in network dynamics rather than absolute signal magnitude [31].

Although the strongest associations were observed over occipital regions (O1/O2), these channels are typically associated with visual cortical activity. Alternative explanations should therefore be considered. Residual visual processing or uncontrolled visual input during EEG recording may influence occipital activity, even under eyes-closed resting conditions. However, all recordings were conducted under standardized resting-state conditions with eyes closed and minimal external stimulation. This protocol reduces the likelihood that the observed effects were driven solely by visual confounds. Instead, the observed occipital changes may reflect broader cortical reorganization and network-level redistribution associated with post-stroke recovery.

Slow-frequency activity, particularly in the delta band, has been widely associated with post-stroke neural dysfunction and recovery-related cortical reorganization [32]. Previous quantitative EEG studies have also shown that low-frequency cortical activity and slow–fast spectral balance are closely associated with functional outcomes after stroke [33, 34]. In the present study, changes in relative delta power showed a strong negative correlation with improvements in FMA-UE scores. This finding suggests that reduced relative delta dominance may reflect recovery-related normalization or redistribution of cortical activity.

These findings demonstrate a clear dissociation between EEG features that predict treatment responsiveness and those that track recovery-related neural changes. Baseline beta-band activity in temporal–sensorimotor regions was the most informative feature for predicting treatment responsiveness. Previous studies have shown that neurophysiological measures of motor cortical function are associated with recovery potential and clinical motor outcomes after stroke [35, 36]. In other words, these findings suggest that baseline predictive features reflect the pre-existing functional state of motor-related cortical networks. In contrast, longitudinal changes in relative delta-band power over posterior regions were associated with functional improvement during rehabilitation [30]. These changes may reflect ongoing cortical adaptation and large-scale network reorganization during recovery. These results indicate that predictive biomarkers and recovery-tracking biomarkers capture distinct aspects of post-stroke neural dynamics.

This distinction has important implications for the use of EEG in stroke rehabilitation. Baseline EEG features may facilitate patient stratification and prediction of treatment responsiveness, whereas longitudinal EEG changes may provide insight into neuroplastic processes and enable monitoring of recovery trajectories. Interestingly, both the baseline predictive biomarker (T3) and the longitudinal recovery biomarker (O1) were located in sensory-related cortical regions rather than canonical motor areas. This observation suggests that treatment responsiveness and motor recovery following NIBS may involve broader sensory–motor network reorganization beyond

primary motor cortex. By integrating machine learning with longitudinal statistical analysis, the present study provides a framework that links predictive modeling with physiologically meaningful interpretation. This framework highlights the potential of EEG as both a predictive and recovery-tracking biomarker for personalized rehabilitation strategies. Despite the small sample size, the consistency between machine learning–based feature importance and longitudinal statistical findings strengthens confidence in the identified biomarkers.

Several limitations of this study should be acknowledged. First, the relatively small sample size may limit the generalizability of the findings and reduce the statistical power to detect subtle associations between EEG features and motor recovery. Second, the number of longitudinal EEG recordings was limited, restricting a detailed assessment of long-term neural dynamics and the persistence of NIBS-related effects. Future studies should address these limitations by validating the proposed EEG biomarkers in larger, multi-center cohorts with extended follow-up periods. Increasing the number of longitudinal recordings would enable a more comprehensive characterization of recovery trajectories and neural reorganization over time. Future studies should also evaluate subject-independent validation strategies, such as leave-one-subject-out cross-validation, to better assess model generalizability in small-sample clinical settings. In addition, integrating EEG spectral features with functional connectivity measures and clinical variables may further improve predictive performance and enhance the clinical applicability of EEG-based biomarkers for personalized stroke rehabilitation.

5 Conclusion

This study identified distinct EEG-based biomarkers for predicting and tracking motor recovery following NIBS in patients with subacute stroke by combining machine learning with longitudinal statistical analysis. Baseline beta-band activity in the temporal region, particularly at T3, was the most informative feature for predicting treatment responsiveness. These findings indicate that pre-intervention EEG may provide clinically useful information for patient stratification. In contrast, longitudinal recovery was associated with changes in relative delta-band power over posterior regions. The strongest association was observed at O1. These changes may reflect ongoing neuroplastic reorganization during rehabilitation.

These findings demonstrate that baseline predictive biomarkers and longitudinal recovery-tracking biomarkers capture distinct aspects of post-stroke neural dynamics. This distinction has important clinical implications and supports a two-stage framework in which EEG can be used both to identify patients who are likely to respond to intervention and to monitor neurophysiological changes during recovery. The present study highlights the potential of EEG as a practical and non-invasive tool for guiding personalized rehabilitation strategies in stroke rehabilitation.

Declarations

- Funding : This work was partly supported by the National Research Foundation of Korea(NRF) grant funded by the Korea government(MSIT) (No. RS-2024-00336880; RS-2025-23963510). The funding body had no role in the design of the study; in the

collection, analysis, or interpretation of data; or in writing the manuscript or the decision to publish.

- Conflict of interest/Competing interests : The authors declare that they have no competing interests.
- Ethics approval and consent to participate : This study was approved by the Institutional Review Board (IRB) of Samsung Medical Center (approval no. SMC 2013-06-002). All experimental procedures were conducted in accordance with the relevant guidelines and regulations. Written informed consent was obtained from all participants or their legal guardians prior to participation.
- Consent for publication : Not applicable.
- Data availability : The datasets generated and/or analyzed during the current study are not publicly available due to patient privacy and ethical restrictions, but are available from the corresponding author on reasonable request.
- Materials availability : Not applicable.
- Code availability : The code used in this study is available from the corresponding author on reasonable request.
- Author contribution : Han contributed to software implementation, data analysis, and visualization, and drafted the manuscript. Huh contributed to software implementation, validation, and manuscript review and editing. Sang Wook Lee contributed to validation and manuscript review and editing. Kim contributed to conceptualization, data collection, and resource provision, and participated in manuscript review and editing. Minji Lee conceptualized the study, developed the methodology, supervised the project, and contributed to data curation and manuscript review and editing. All authors read and approved the final manuscript.

References

[1] GBD 2019 Stroke Collaborators: Global, regional, and national burden of stroke and its risk factors, 1990–2019: a systematic analysis for the global burden of disease study 2019. Lancet Neurol. **20**(10), 795–820 (2021)

[2] Ward, N.S., S.J., F.R.: The functional anatomy of cerebral reorganisation after focal brain injury. J. Physiol. **99**, 425–436 (2006) https://doi.org/10.1016/j.jphysparis.2006.03.002

[3] Du, J., Tian, L., Liu, W., Hu, J., Xu, G., Ma, M., Fan, X., Ye, R., Jiang, Y., Yin, Q., Zhu, W., Xiong, Y., Yang, F., Liu, X.: Effects of repetitive transcranial magnetic stimulation on motor recovery and motor cortex excitability in patients with stroke: a randomized controlled trial. Eur. J. Neurol. **23**, 1666–1672 (2016)

[4] Marquez, J., Vliet, P., McElduff, P., Lagopoulos, J., Parsons, M.: Transcranial direct current stimulation (tDCS): Does it have merit in stroke rehabilitation? a systematic review. Int. J. Stroke **10**, 306–316 (2015)

[5] Wang, C., Chen, Y., Song, P., Yu, H., Du, J., Zhang, Y., Sun, C.: Varied response of eeg rhythm to different tDCS protocols and lesion hemispheres in stroke

subjects with upper limb dysfunction. J. Neuroeng. Rehabil. **18**, 120 (2021)

[6] Lee, M., Park, W., Park, E., Kweon, S., Kim, Y.: Neuromodulation effect according to lesion location after dual-mode brain stimulation in patients with subacute stroke: A preliminary study. Appl. Sci. **14** (2024) https://doi.org/10.3390/app14219636

[7] Lee, M., Kim, Y.-H., Im, C.-H., Kim, J.-H., Park, C.-h., Chang, W.H., Lee, A.: What is the optimal anodal electrode position for inducing corticomotor excitability changes in transcranial direct current stimulation? Neurosci. Lett. **584** (2015)

[8] Vatinno, A.A., Simpson, A., Ramakrishnan, V., Bonilha, H.S., Bonilha, L., Seo, N.J.: The prognostic utility of electroencephalography in stroke recovery: A systematic review and meta-analysis. Neurorehabil. Neural Repair **36**(4-5), 255–268 (2022)

[9] Liao, X.-Y., Jiang, Y.-E., Xu, R.-J., Qian, T.-T., Liu, S.-L., Che, Y.: A bibliometric analysis of electroencephalogram research in stroke: current trends and future directions. Front. Neurol. **16** (2025) https://doi.org/10.3389/fneur.2025.1539736

[10] Lee, M., Park, H.-Y., Park, W., Kim, K.-T., Kim, Y.-H., Jeong, J.-H.: Multi-task heterogeneous ensemble learning-based cross-subject EEG classification under stroke patients. IEEE Trans. Neural Syst. Rehabil. Eng. **32** (2024)

[11] Min, Y.-S., Park, J.W., Jang, K.E., Lee, H.J., Lee, J., Lee, Y.-S., Jung, T.-D., Chang, Y.: Power spectral density analysis of long-term motor recovery in patients with subacute stroke. Neurorehabil. Neural Repair **33**(1), 38–46 (2019)

[12] Montecinos, C., Espinoza, J., Zapata, M.Z., Meruane, V., Fernandez, R.: Improving fast EMG classification for hand gesture recognition: A comprehensive analysis of temporal, spatial, and algorithm configurations for healthy and post-stroke subjects. Sensors **25** (2025) https://doi.org/10.3390/s25226980

[13] Lee, M., Kim, Y.-H., Lee, S.-W.: Motor impairment in stroke patients is associated with network properties during consecutive motor imagery. IEEE Trans. Biomed. Eng. **69**(8) (2022)

[14] Lanzone, J., Motolese, F., Ricci, L., Tecchio, F., Tombini, M., Zappasodi, F., Cruciani, A., Capone, F., Lazzaro, V.D., Assenza, G.: Quantitative measures of the resting EEG in stroke: a systematic review on clinical correlation and prognostic value. Neurol. Sci. (2023) https://doi.org/10.1007/s10072-023-06981-9

[15] Jiang, L., Ding, H., Ma, Q., Gao, S., Zhang, X., Chun, B.: Comparing the effectiveness of different exercise interventions on quality of life in stroke patients: a randomized controlled network meta-analysis. BMC Neurol. **25** (2025) https://doi.org/10.1186/s12883-025-04035-5

[16] Lanzone, J., Colombo, M.A., Sarasso, S., Zappasodi, F., Rosanova, M., Massimini, M., Lazzaro, V.D., Assenza, G.: EEG spectral exponent as a synthetic index for the longitudinal assessment of stroke recovery. Clin. Neurophysiol. **137**, 92–101 (2022)

[17] Timothy, S., Leigh, L.J., Bryan, K.: Experience-associated structural events, subependymal cellular proliferative activity, and functional recovery after injury to the central nervous system. J. Cereb. Blood Flow Metab. **20**, 1513–1528 (2000)

[18] Huynh, B.P., DiCarlo, J.A., Vora, I., Ranford, J., Gochyyev, P., Lin, D.J., Kimberley, T.J.: Sensitivity to change and responsiveness of the upper extremity Fugl-Meyer Assessment in individuals with moderate to severe acute stroke. Neurorehabil. Neural Repair **37**(8), 545–553 (2023)

[19] Kwon, T.G., Park, E., Kang, C., Chang, W.H., Kim, Y.-H.: The effects of combined repetitive transcranial magnetic stimulation and transcranial direct current stimulation on motor function in patients with stroke. Restor. Neurol. Neurosci. **34**(6), 915–923 (2016)

[20] Park, W., Kim, Y., Kim, S., Kim, L.: EEG patterns of subacute stroke patients performing motor tasks correlate with motor functional outcome: Preliminary results. Proc. IEEE Eng. Med. Biol. Soc. (EMBC), 4674–4677 (2016)

[21] Dobkin, B.H.: Strategies for stroke rehabilitation. Lancet Neurol. **3**(8), 485–491 (2004)

[22] Las, M., Dalise, S., Privitera, L., Giannini, N., Mancuso, M., Azzollini, V., Ciapetti, T., Grippo, A., Micera, S., Cecchi, F., Mazzoni, A., Chisari, C., Bandini, A.: Enhancing upper limb motor recovery prediction after acute stroke using EEG and subacute data. APL Bioeng. **10** (2026) https://doi.org/10.1063/5.0287165

[23] Muthukumaraswamy, S.D.: High-frequency brain activity and muscle artifacts in MEG/EEG: a review and recommendations. Front. Hum. Neurosci. **7**(138) (2013)

[24] Pfurtscheller, G., Da Silva, F.L.: Event-related EEG/MEG synchronization and desynchronization: basic principles. Clin. Neurophysiol. **110**(11), 1842–1857 (1999)

[25] Finnigan, S., Van Putten, M.J.: EEG in ischaemic stroke: quantitative EEG can uniquely inform (sub-) acute prognoses and clinical management. Clin. Neurophysiol. **124**(1), 10–19 (2013)

[26] Palva, J.M., Wang, S.H., Palva, S., Zhigalov, A., Monto, S., Brookes, M.J., Schoffelen, J.-M., Jerbi, K.: Ghost interactions in MEG/EEG source space: A note of caution on inter-areal coupling measures. NeuroImage **173** (2018)

[27] Setiawan, H., Islamiyah, W.R., Wibawa, A.D., Purnomo, M.H.: Identifying EEG

parameters to monitor stroke rehabilitation using individual analysis. Proc. Int. Semin. Intell. Technol. Appl. (ISITIA) (2019)

[28] Tang, C.-W., Hsiao, F.-J., Lee, P.-L., Tsai, Y.-A., Hsu, Y.-F., Chen, W.-T., Lin, Y.-Y., Stagg, C.J., Lee, I.-H.: β-oscillations reflect recovery of the paretic upper limb in subacute stroke. Neurorehabil. Neural Repair **34**(5), 450–462 (2020)

[29] Ding, L., Tian, X., Ren, H., Chen, Z., Shu, X., Chen, S., Jia, J.: Resting-state EEG associated with clinical measures to predict upper limb motor recovery of subacute stroke. Front. Neurol. **16** (2025) https://doi.org/10.3389/fneur.2025.1577393

[30] Chang, J.: Test-retest reliability of single spectral power and spectral power ratios in relative and absolute values. Brain Behav. **15**(11) (2025)

[31] Maria Concetta Pellicciari a, S.B., Ponzo, V., Cinnera, A.M., Mancini, M., Casula, E.P., Sallustio, F., Paolucci, S., Caltagirone, C., Koch, G.: Dynamic reorganization of TMS-evoked activity in subcortical stroke patients. NeuroImage **175** (2018)

[32] Ramanathan, D.S., Ling Guo, T.G., Davidson, G., Hishinuma, A.K., Won, S.-J., Knight, R.T., Chang, E.F., Swanson, R.A., Ganguly, K.: Low frequency cortical activity is a neuromodulatory target that tracks recovery after stroke. Nat. Med. **24**(8) (2018)

[33] Zhang, Y., Chu, H., Qiao, Q., Dong, S., Liu, J., Wang, H.: Prospective analysis of quantitative EEG indices for predicting functional outcomes in acute ischemic stroke. SLAS Technol. **33** (2025) https://doi.org/10.1016/j.slast.2025.100317

[34] Finnigan, S., Wong, A., Read, S.: Defining abnormal slow EEG activity in acute ischaemic stroke: Delta/alpha ratio as an optimal qEEG index. Clin. Neurophysiol. **127**, 1452–1459 (2016)

[35] Tozlu, C., Edwards, D., Boes, A., Labar, D., Tsagaris, K.Z., Silverstein, J., Lane, H.P., Sabuncu, M.R., Liu, C., Kuceyeski, A.: Machine learning methods predict individual upper limb motor impairment following therapy in chronic stroke. Neurorehabil. Neural Repair **34**(5) (2020)

[36] Maura, R.M., Parra, S.R., Stevens, R.E., Weeks, D.L., Wolbrecht, E.T., Perry, J.C.: Literature review of stroke assessment for upper-extremity physical function via EEG, EMG, kinematic, and kinetic measurements and their reliability. J. Neuroeng. Rehabil. **20**(21) (2023)

Supplementary Files

This is a list of supplementary files associated with this preprint. Click to download.

- JNER2026YRHuhHJHanSupplementarymaterial.pdf